ChemComm

Accepted Manuscript

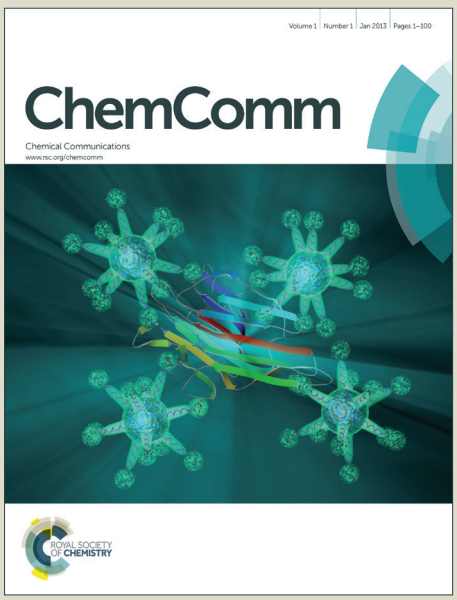

ROYAL SOCIETY OF CHEMISTRY

www.rsc.org/chemcomm

Cite this: DOI: 10.1039/c0xx00000x

www.rsc.org/xxxxxx

ARTICLE TYPE

Hierarchical meso-macroporous poly(ionic liquid) monolith derived from single soft template

Chenjue Gao, Guojian Chen, Xiaochen Wang, Jing Li, Yu Zhou*, Jun Wang*

Received (in XXX, XXX) XthXXXXXXXXX 20XX, Accepted Xth XXXXXXXXX 20XX

DOI: 10.1039/b000000x

Hierarchical meso-macropores poly(ionic liquid) monolith with tunable pore structure is synthesized through free radical self-polymerization of 1-allyl-3-vinylimidazolium ionic liquid by using the tri-block copolymer P123 as the soft template. The obtained polymeric matrix can highly disperse heteropolyanion through anion-exchange, exhibiting superior catalytic activity in cis-cyclooctene epoxidation with H_2O_2.

Mesoporous poly(ionic liquid)s (MPILs) simultaneous combine the features of mesoporous materials, polymers and ionic liquids (ILs) (large surface area, adjustable pore structure, versatile organic framework, non-volatility, superior ionic conductivity, etc.)[1,2], providing numerous new functionality that can be applied in the fields of adsorption, separation, catalysis and so on.[3-7] The practical performances of MPILs are closely related to their pore structures, which motivates the development of various pore formation strategies.[8-12] However, MPILs are synthesized through self-assembly process[9,10] (except the one example of hard-templating route[11]), and have never been achieved through a soft-templating pathway.

The soft template approach is facile and efficient to fabricate and continuous control the mesostructure, especially able to generate suitable pore structure on the materials that are normally nonporous in a template-free route.[13-19] Though soft template has been widely used in the fabrication of inorganic or inorganic-organic hybrid mesoporous materials,[13-16] it is rarely applied in the pure organic mesoporous polymers due to the difficulty in template removal.[17-19] During the synthesis of pure organic mesoporous materials, the template removal relies on the solvent extraction route while calcination usually causes the damage of the framework before removing the template.[20,21] Therefore, balancing the interaction between the template and organic precursor is crucial to enable the polymerization around the template with suitable bind force, which avoids close conjunction of the organic compounds and thus makes it possible to remove the template by solvent extraction.[22]

Herein, we report for the first time the soft template synthesis of MPILs by radical self-polymerization of the 1-allyl-3-vinylimidazolium-IL monomer. The obtained MPILs materials exhibit hierarchical meso-macroporous structure and monolithic macro-morphology, which is derived from the soft template of tri-block copolymer P123 ($EO_{20}PO_{70}EO_{20}$). To the best of our knowledge, reports on dual porous MPILs have not appeared so far. After removing P123, the anion-exchange property of this material allows facile tuning of counter anions, through which the Keggin-structured phosphotungstic anion is exchanged and highly dispersed onto the surface of mesopores. The resulting sample acts as an efficient heterogeneous catalyst for H_2O_2-mediated epoxidation of cis-cyclooctene.

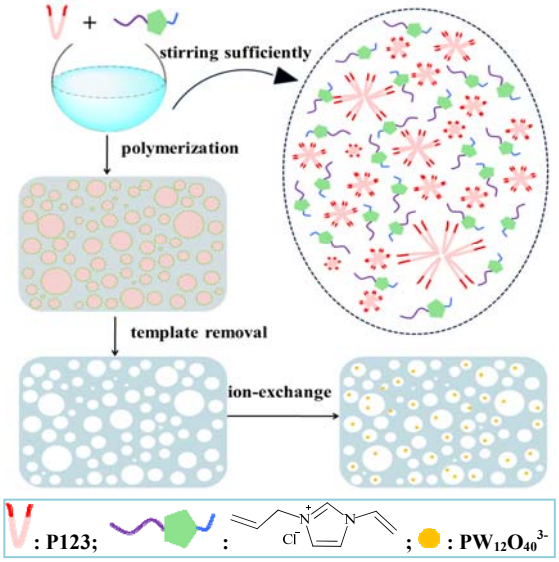

Scheme 1. Synthetic process for hierarchical meso-macroporous poly(ionic liquid) by using the soft template P123.

Scheme 1 illustrates the synthetic process for the hierarchical meso-macroporous poly(ionic liquid), shorten as HMP(*x*) (*x* is index of weight amount (g) of P123 in synthetic compositions). The synthesis involves dissolving P123 in water to get a micelle solution and the succeeding dissolution of the IL precursor with long time stirring to enable the sufficient interaction between P123 and IL. According to the charge matching principle for synthesizing mesoporous materials with a template, the IL cationic precursor interacts with P123 through the $S^0H^+X^-I^+$ mode (S^0: nonionic surfactant P123, H^+: hydrogen ions of ionization, X^-: IL anion, I^+: IL cation),[23,24] in which the H^+ concentration will increase after introduction of the initiator ammonium persulfate (APS). The synthesis starts at a relative high temperature for facilitating decomposition of the initiator APS and polymerization occurs with ongoing of the temperature program (first at T_1 for 10 h and then T_2 for 14 h). The template P123 is removed by extracting the as-synthesized material in ethanol.

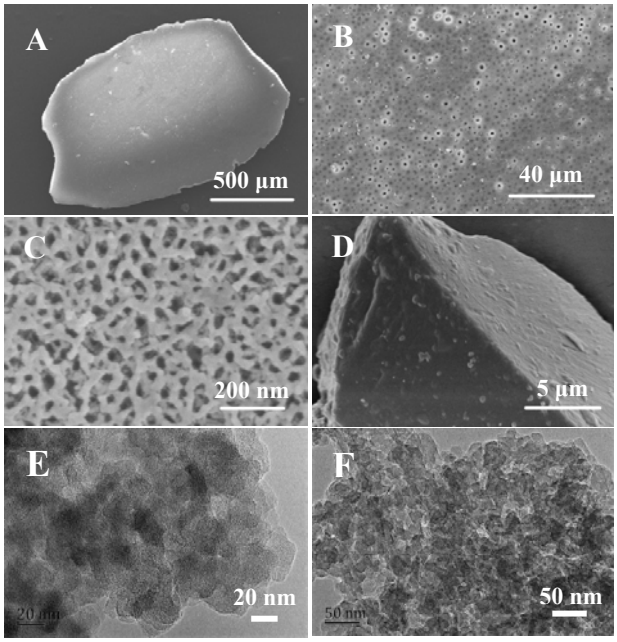

Figure 1. SEM images of HMP(3) (A-C) and HMP(0) (D); and TEM images of HMP(3) (E and F).

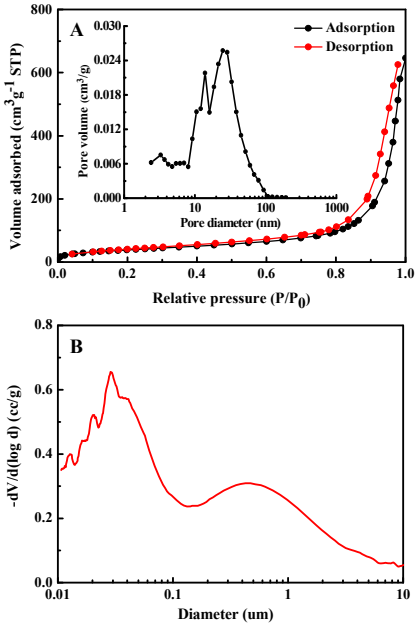

Figure 2. Pore structure of HMP(3). (A) nitrogen sorption isotherm with mesopore size distribution (inset); (B) macropore size distribution detected by mercury inclusion porosimetry.

The SEM images of the typical sample HMP(3) (Figure 1A-C) present a clear hierarchical porous structure. The macroscopic shape is monolith in millimeter or centimeter scales. Abundant macropores with the diameter in micrometer level are observed by magnifying the surface of the monolith. The primary particles are nano-sticks with the width of around 20 nm and the length ranging tens of nanometers; they are intertwined with each other to form a cross-linked framework and corresponding mesoporous structure, which is further confirmed by the TEM images (Figure 1E and F). On the contrary, the sample synthesized in the absence of the soft template P123 under otherwise similar conditions only shows smooth particle surface without any meso or macropores observed (Figure 1D), implying the crucial role of P123 in creating the pore structure. Moreover, Fourier transform infrared (FTIR) (Figure S1), ^{1}H and ^{13}C MAS NMR spectra (Figure S2) for this material and its nonporous counterpart prove the successful polymerization of the IL monomer while the presence of P123 should have not hamper the formation of the polymer matrix. The elemental analysis (Table S1) indicates that the molar ratio of C to N in the HMP material is 4 after template removal, same as the value in the IL monomer and the nonporous counterpart. The result suggests that in this work the soft template P123 can be completely removed through the solvent extract. The detection of S element may arise from the partial anion-exchange with the SO_4^{2-} (Table S1) formed during the decomposition of APS. The thermogravimetric (TG) analysis under oxygen atmosphere (Figure S3) reveals that the porous HMP material bears the thermal stability up to ca. 240 °C, as high as its nonporous counterpart. All the above features allow drawing that the existence of P123 not only does not disturb the polymerization process, but also acts as a facilely removable soft template that is responsible for the formation of hierarchical meso-macropores.

The quantitative analysis of the pore structure of above HMP sample is conducted with nitrogen sorption and mercury inclusion porosimetry. The isotherm is type IV with a clear hysteresis loop of type H4 at the high relative pressure (P/P_0) range from 0.9 to 0.99 (Figure 2A), reflecting a typical mesostructure. The BET (Brunauer-Emmett-Teller) surface area and total pore volume are 143 $m^2\ g^{-1}$ and 0.94 $cm^3\ g^{-1}$, respectively. The most probable distribution in mesopores appears at ca. 26 nm (Figure 2A, inset), in good accordance with the SEM and TEM images. The macropore size distribution (Figure 2B and S4) indicates that the porosity degree of HMP(3) is 55.5%, giving pore size distribution from nanometer to micrometer. Two peaks are observed at ca. 28 nm and 0.5 μm, agreeing with nitrogen sorption, SEM and TEM results, which prove the hierarchical meso-maroporous structure. Besides, P123 solutions before and after addition of IL are characterized by dynamic light scattering and TEM to understand the formation mechanism of the hierarchical meso-macroporous structure over these MPILs (Figure S5 and S6).

Table 1. Textural properties of HMP(x) series materials synthesized with the initial composition containing P123 (x g), [AVIm]Cl (1.7 g), H_2O (8 g) and APS (7 g). [a]

HMP(x) [b]	S_{BET} [c] ($m^2\ g^{-1}$)	V [d] ($cm^3\ g^{-1}$)	D_{av} [e] (nm)
HMP(0)	1	-	-
HMP(0.5)	44	0.26	23.7
HMP(1)	90	0.61	27.2
HMP(2)	130	1.04	31.9
HMP(3)	144	0.94	26.0
HMP(4)	122	0.58	18.8

[a] These samples are synthesized by polymerization firstly at 38 °C for 10 h then at 50 °C for 14 h; [b] These samples are denoted as HMP(x), in which x is index of the weight amount (g) of P123 added in synthetic compositions; [c] BET surface area; [d] Total pore volume; [e] Average pore diameter.

Table 2. Textural properties and catalytic performances of heteropolyanion-loaded HMP series catalysts in the epoxidation of *cis*-cyclooctene with H_2O_2. [a]

Entry	Catalyst	S_{BET} [b] ($m^2\ g^{-1}$)	V [c] ($cm^3\ g^{-1}$)	D_{av} [d] (nm)	Conversion [e] (%)	Selectivity [f] (%)	TOF (h^{-1})
1	H_3PW	5	-	-	23	86	35
2	IL-PW	5	-	-	22	91	33
3	PW@HMP(0)	7	0.03	-	26	99	39
4	PW@HMP(0.5)	35	0.17	19.1	90	99	134
5	PW@HMP(1)	54	0.21	15.5	97	99	145
6	PW@HMP(3)	65	0.23	14.4	99	99	148

[a] Reaction conditions: cis-cyclooctene (5 mmol), H_2O_2 (4 mmol, 30 wt%), methanol (1 mL, as the solvent), 60°C, 4 h; [b] BET surface area; [c] Total pore volume; [d] Average pore size; [e] Conversion based on H_2O_2; [f] Selectivity for 1,2-epoxycyclooctane; by-products: 2-cycloocten-1-ol, 2-cycloocten-1-one and 1,2-cy-clooctanediol.

Various influence factors are studied to control the pore structure of HMP series materials. One significant parameter is the template concentration in the initial solution. Nitrogen sorption results (Figure S7) indicate that the samples synthesized using different amounts of P123 all give up to type IV isotherms and wide pore size distribution curves with the most probable pore sizes of 20-30 nm. Table 1 lists the textural properties of these materials. In the absence of P123, the extremely low BET surface of ca. 1 $m^2\ g^{-1}$ is indicative of nonporous structure, consistent with the SEM illustration. The small amount of P123 (x= 0.5 g) causes a low surface area of 43 $m^2\ g^{-1}$ with the pore volume of 0.26 $cm^3\ g^{-1}$. The surface area and pore volume continuously increase with P123 amounts, achieving the maximum value as using 3 g P123. Further enhancement of the template added results in a slight decline in mesopores. The influence of IL concentration is similar to the template effect (Table S2, entry 1-4, Figure S8) and the maximum surface area is achieved with a relative high IL amount, while a too low IL concentration leads to a low surface area. It is thus proposed that only suitable P123 and IL concentrations can benefit the assembly of the organic precursor around the template. Influences of water amount (Table S2, entry 5-8, Figure S9) and polymerization temperature (Table S2, entry 9-16, Figure S10) are explored and the results indicate that HMPs with high surface areas can be synthesized in a wide range. Besides, no solid is obtained by varying the counter anion of the IL monomer to be PF_6^-, and MPILs with smaller surface areas are synthesized using [AVIm]Br and [AVIm]BF_4 (Table S2, entry 17, 18, Figure S11). The result suggests that the counter anions significantly affect the pore formation,[25,26] which may be attributable to that the counter anions should have altered the $S^0H^+X^-I^+$ interaction between the template and the IL precursor (detailed discussion in the footnote of Table S2).[22]

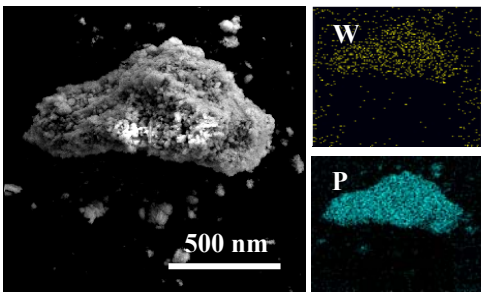

Figure 3. Energy-dispersive X-ray spectrometry (EDS) elemental mapping analysis of the sample PW@HMP(3).

The MPILs possess repeated IL units in the polymer matrix; therefore, through anion-exchange, the counter anions can be facilely tailored to access versatile functions. In this work, HMP materials are utilized as the supports towards polyoxometalate (POM) based heterogeneous catalysts. POMs have been widely used as the catalysts for various organic reactions due to acid/base and redox properties. IL-cations have been used to pair with heteropolyanions for preparing diversified ionic liquid-based polyoxometalate (IL-POM) hybrid catalysts.[27-29] However, those hybrids usually possess inferior surface areas or nonporous structures, inhibiting the mass transfer in heterogeneous catalytic reaction media. To overcome above shortness, we explore the application of our newly obtained HMPs to prepare POM-based heterogeneous catalysts, with the phosphotungstic anion $PW_{12}O_{40}^{3-}$ (PW) being ion-exchanged into the matrix of HMP(x) (x= 0, 0.5, 1 and 3, synthetic conditions for HMP(x) are in caption of Table 1) for obtaining the catalysts PW@HMP(x). Their structural characterizations (Figures 3 and S12-14) validate the successful immobilization of PW species and the well retain of the mesostructure.

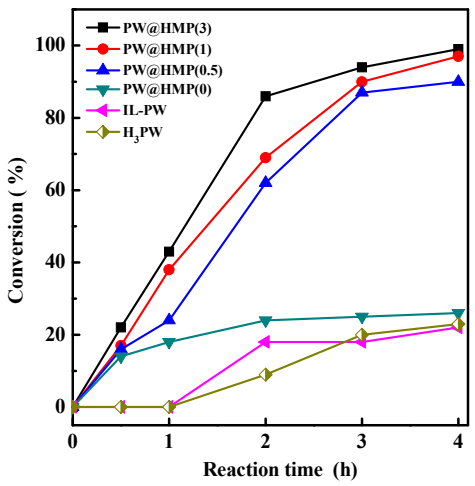

Figure 4. Conversion of *cis*-cyclooctene as a function of reaction time for PW@HMP(x)-catalyzed liquid-phase epoxidation with H_2O_2. Reaction conditions: cis-cyclooctene (5 mmol), H_2O_2 (4 mmol, 30 wt%), methanol (1 mL, as the solvent), 60 °C, 4 h.

Table 2 summarizes catalytic performances of PW@HMP(x) series in liquid-phase epoxidation of cis-cyclooctene with H_2O_2. Phosphotungstic acid $H_3PW_{12}O_{40}$ (H_3PW) is a homogeneous

catalyst in this reaction and gives a relative low conversion of 23% (based on H_2O_2) (entry 1). The control hybrid catalyst IL-PW prepared by pairing the PW anion with IL-cation of [AVIm]Cl performances heterogeneously, with also a low conversion of 22% (entry 2). In contrast, the series catalysts of PW@HMP(x) all demonstrate high conversions (entry 3-6). The kinetic plots (Figure 4) further illustrate that the large-surface-area catalyst explicitly accelerates the reaction throughout the catalytic process. Moreover, the PW@HMP(*x*) materials give the turnover frequency (TOF) up to 148 h^{-1}, much higher than those over the IL-POM counterpart or the previous IL-functionalized POM-based materials.[30,31] The investigation on the effect of substrate amounts shows the high conversion of 93% even using the ideal equimolar of H_2O_2 and cis-cyclooctene (Figure S15), implying not only the high activity of the catalysts PW@HMP(*x*) but also efficient utilization of H_2O_2. In catalysis, the mesoporosity accounting for the high specific surface area benefits the loading and well dispersion of the active PW species as well as the accessibility of substrates to active sites, while both meso and macropores favour the improvement of mass transport. The catalyst recycling test (Figure S16) indicates that the catalyst can be directly reused after facile separation by filtration. Characterizations for the reused catalyst (Figure S17-19) demonstrate the retaining of composition and porous structure for the reused catalyst, which accounts for the quite steady catalyst reuse. The slight decline of activity after the third recycling run may be ascribed to the possible degradation of PW anion in the presence of H_2O_2.[32]

In summary, soft-templating approach is for the first time applied to successfully synthesize hierarchical meso-macroporous poly(ionic liquid) materials by using the single template of P123. The pore structures of the obtained HMP materials can be adjusted by varying the elemental synthetic parameters, such as the concentrations of template and IL precursor, etc. Owing to the special property of the IL-like unit in mesoporous polymer matrix, the present materials can be facilely functionalized through exchanging the guest anions. The thus prepared heteropolyanion-loaded HMP materials behave as the recyclable heterogeneous catalysts with superior activity in liquid-phase epoxidation of cis-cyclooctene with H_2O_2.

This work was supported by the National Natural Science Foundation of China (Nos. 21303038, 21136005 and 21476109), Jiangsu Province Science Foundation for Youths (No. BK20130921), Specialized Research Fund for the Doctoral Program of Higher Education (No. 20133221120002), and the Project of Priority Academic Program Development of Jiangsu Higher Education Institutions (PAPD). We also thank Dr. Luming Peng and Mr. Meng Wang from College of Chemistry and Chemical Engineering of Nanjing University for conducting and analyzing the solid-state ^1H and ^{13}C MAS NMR.

Notes and references

State Key Laboratory of Materials-Oriented Chemical Engineering, College of Chemistry and Chemical Engineering, Nanjing Tech University (former Nanjing University of Technology), Nanjing 210009, Jiangsu, P. R. China

**Corresponding author, E-mail: njutzhouyu@njtech.edu.cn (Y. Zhou), junwang@njtech.edu.cn (J. Wang); Tel: +(86) 25-83172264.*

† Electronic Supplementary Information (ESI) available: [Experimental section, Tables S1 and S2, and Figures S1~S12]. See DOI: 10.1039/b000000x/

1 H. Sai, K. W. Tan, K. Hur, E. Asenath-Smith, R. Hovden, Y. Jiang, M. Riccio, D. A. Muller, V. Elser, L. A. Estroff, S. M. Gruner and U. Wiesner, *Science.*, 2013, **341**, 530−534.
2 J. Y. Yuan, D. Mecerreyes and M. Antonietti, *Prog. Polym. Sci.*, 2013, **38**, 1009−1036.
3 D. Mecerreyes, *Prog.Polym. Sci.*, 2011, **36**, 1629–1648.
4 G. Yu, Q. Li, N. Li, Z. Man, C. Pu, C. Asumana and X. Chen, *Polym Eng Sci.*, 2014, **54**, 59–63.
5 F. J. Liu, S. F. Zuo, W. P Kong and C. Z. Qi,*Green Chem.*, 2012, **14**, 1342−1349.
6 S. Ghazali-Esfahani, H. B. Song, E. Păunescu, F. D. Bobbink, H. Z. Liu, Z. F. Fei, G. Laurenczy, M. Bagherzadeh, N. Yan and P. J. Dyson, *Green Chem.*, 2013,**15**, 1584−1589.
7 D. Chandra and A. Bhaumik, *J. Mater. Chem.*, 2009, **19**, 1901–1907.
8 D. C. Wu, F. Xu, B. Sun, R. W. Fu, H. K. He and K. Matyjaszewski, *Chem. Rev.*, 2012, **112**, 3959−4015.
9 Q. Zhao, P. F. Zhang, M. Antonietti and J. Y. Yuan, *J. Am. Chem. Soc.*, 2012, **134**, 11852−11855.
10 S. Soll, Q. Zhao, J. Weber and J. Y. Yuan, *Chem. Mater.*, 2013, **25**, 3003−3010.
11 A. Wilke, J. Y. Yuan, M. Antonietti and J. Weber, *ACS. Macro .Lett.*, 2012, **1**, 1028−1031.
12 C. Boyère, A. Favrelle, A. F. Léonard, F. Boury, C. Jérôme and A. Debuigne, *J. Mater. Chem. A.*, 2013, **1**, 8479-8487.
13 C. Q. Liu, J. B. Lambert and L. Fu, *J. Am. Chem. Soc.*, 2003, **125**, 6452−6461.
14 D. H. Chen, Z. Li, C. Z. Yu, Y. F. Shi, Z. D. Zhang, B Tu and D. Y. Zhao, *Chem. Mater.*, 2005, **17**, 3228–3234.
15 D. Y. Zhao, J. L. Feng, Q. S. Huo, N. Melosh, G. H. Fredrickson, B. F. Chmelka and G. D. Stucky, *Science.*, 1998, **279**, 548–552.
16 T. Y. Chen, B. Y. Du and Z. Q. Fan, *Langmuir.*, 2012, **28**, 15024−15032.
17 J. Jang and J. Bae, *Chem. Commun.*, 2005, **9**, 1200–1202.
18 Y. R. Liang, R. W. Fu and D. C. Wu, *ACS Nano.*, 2013, **7**, 1748–1754.
19 L. Peng, J. L. Zhang, S. L. Yang, B. X. Han, X. X. Sang, C. C. Liu and G. Y. Yang, *Chem. Commun.*, 2014, **50**, 11957–11960.
20 M. Hillmyer, P. Lipic, D. Hajduk, K. Almdal and F. Bates, *J. Am. Chem. Soc.*, 1997, **119**, 2749–2750.
21 P. Lipic, F. Bates and M. Hillmyer, *J. Am. Chem. Soc.*, 1998, **120**, 8963–8970.
22 Y. Meng, D. Gu, F. Q. Zhang, Y. F. Shi, L. Cheng, D. Feng, Z. X. Wu, Z. X. Chen, Y. Wan, A. Stein and D. Y. Zhao, *Chem. Mater.*, 2006, **18**, 4447–4464.
23 Q. Huo, D. Margolese and U. Ciesla, *Nature*, 1994, **368**, 317–321.
24 G. Soler-Illia, C. Sanchez, B. Lebeau and J. Patarin, *Chem. Rev.*, 2002, **102**, 4093–4138.
25 H. P. Lin, C. P. Kao, C. Y. Mou and S. B. Liu, *J. Phys. Chem. B,* 2000, **104**, 7885-7894.
26 S. Che, S. Lim, M. Kaneda, H. Yoshitake, O.Terasaki and T. Tatsumi, *J. Am. Chem. Soc.*, 2002, **124**, 13962–13963.
27 Y. Zhou, G. J. Chen, Z. Y. Long and J. Wang, *RSC Adv.*, 2014, **4**, 42092–42113.
28 Y. Leng, J. Wang, D. R. Zhu, X. Q. Ren, H. Q. Ge and L. Shen, *Angew. Chem. Int. Ed.*, 2009, **48**, 168–171.
29 G. J. Chen, Y. Zhou, Z. Y. Long, X. C. Wang, J. Li and J. Wang, *ACS Appl. Mater.*, 2014, **6**, 4438−4446.
30 G. J. Chen, Y. Zhou, P. P. Zhao, Z. Y. Long and J. Wang, *ChemPlusChem.*, 2013, **78**, 561–569.
31 Y. Leng, J. Wang, D. Z. Zhu, M. Zhang, P. P. Zhao, Z. Y. Long and J. Huang, *Green Chem.*, 2011, **13**, 1636–1639.
32 D. C. Duncan, R. C. Chambers, E. Hecht and C. L. Hill, *J. Am. Chem. Soc.*, 1995, 117, 681–691.